

GPS-ASSISTED FEATURE MATCHING IN AERIAL IMAGES WITH HIGHLY REPETITIVE PATTERNS

Gonzalo Luzardo^{†}, Michiel Vlaminck^{*}, Dionysios Lefkaditis[‡], Wilfried Philips^{*}, Hiep Luong^{*}*

^{*} imec-IPI-URC, Ghent University, Sint-Pietersnieuwstraat 41, 9000 Ghent, Belgium

[†]ESPOL Polytechnic University, Km. 30.5 Vía Perimetral, Guayaquil, Ecuador

[‡]SITEMARK, Gaston Geenslaan 11, 3000 Leuven, Belgium

ABSTRACT

Matching aerial images might be challenging when they contain a large number of repetitive patterns. In this paper, we propose a feature-matching method that exploits the use of Affine Oriented FAST and Rotated BRIEF (AORB) as key-point detector and feature descriptor and not accurate GPS (Global Position System) data to achieve a reliable feature matching of nadir UAV images that contain a large number of repetitive patterns. The proposed method assumes that the set of correct matches between two images only differ in a 2D translation. Experimental results show that the proposed method is able to correctly match pairs of very challenging images containing a large number of repetitive patterns.

1. INTRODUCTION

Feature matching compares two sets of points, known as keypoints, from two different but overlapping images. The matching process compares the descriptors of the keypoints in both images and usually includes a filtration step where wrong matches (outliers) are removed from the original set of matches. In the Structure-from-Motion (SfM) pipeline, a low number of correct feature correspondences (inliers) and wrong matches makes the camera pose estimation less reliable and can lead to a wrong or incomplete reconstruction [5]. Matching aerial images is a challenging task mainly because they often contain repetitive structures, such as trees, houses, buildings, crops, solar panels, etc [2].

Descriptors of feature points are commonly based on local image information. Therefore, descriptors from repetitive patterns may not be unique, contributing to a lack of distinction in those regions [4]. This results in a large number of outliers due to local and global ambiguities [3]. In [10], a probabilistic method based on a Bayesian model to remove these outliers by using global, local, and manifold regularizations is proposed. Likewise, a feature matching that assumes that correct matches between two images will only differ in a 2D translation is proposed in [2]. This translation is estimated by computing the so-called pixel-distance histograms on a set of candidate matches. Distinct peaks located in pixel-distance

histograms for X and Y coordinates represent an unknown 2D translation in each coordinate, respectively. More recently, a feature matching method for UAV images that combines the geometric information with the feature similarity is proposed in [8]. Here, the feature matching is restricted in pairwise geometric grid cells to avoid unnecessary feature-similarities computations. Grid cells are defined by matching large-scale SIFT features and selecting the top 10% of them to build the neighborhood pairs that define the grid cells. Although these techniques have shown good performance in matching images with repetitive patterns, their performance decreases when the number of repetitive patterns is larger. Regularizations as a step for filtering outliers proposed in [10] assumes that images contain local structures among neighboring feature points that can be used as local geometrical constraints. However, when the repetitive structures are present on the entire image, this assumption does not hold. Likewise, the repetitive patterns on images can create a large number of peaks in pixel-translation histograms when the method proposed in [2] is used, and a higher peak does not always represent the actual translation. In addition, large-scale SIFT features proposed in [8] will not be able to find unique correct correspondences successfully.

This paper proposes a feature-matching method that overcomes the problems associated with having many repetitive patterns. As in [2], our approach assumes that UAV images are captured so that the set of correct matches between two images only differ in a 2D translation. Additionally, it exploits the use of Oriented FAST and Rotated BRIEF (ORB) extended with affine transformations as keypoint detector and feature descriptor, and GPS (Global Position System) data to achieve a reliable feature matching of nadir oriented UAV images.

2. PROPOSED FEATURE MATCHING

As in [2], our approach is based on estimating a pixel-translation vector between matched keypoints coordinates by using pixel-distance histograms. However, our method is specially tailored to deal with images that contain a large number of repetitive patterns and differs in: (i) it uses AORB

(Affine Oriented FAST and rotated BRIEF) feature extractor and descriptor, (ii) matches are filtered before computing the pixel-distance histograms, and (iii) it uses GPS information to discriminate false peaks in histograms caused by local ambiguities. The pixel-distance histogram is created by computing the coordinate-differences of a set of candidate matches between a pair of images. The pixel shifts differences between the matched keypoints of a pair of images (I_i, I_j) are computed as follows:

$$\Delta_r^k = (r_i^m - r_j^n)^k \quad \Delta_c^k = (c_i^m - c_j^n)^k \quad (1)$$

where $k=1, \dots, N$; N is the number of candidate matches found in the image pair, and (r_i^m, c_i^m) and (r_j^n, c_j^n) are the row and column pixel-coordinates of a m -th and n -th matched keypoints in I_i and I_j , respectively.

Since image pairs are not perfectly aligned, pixel-distance histograms for rows and columns are computed by using bins of size $d > 1$. The value of d depends on the scene depth and how well the images are aligned. Higher values allow dealing with images that are not well aligned, increasing the range so that correct matches with not the same pixel distance belong to the same bin in the histogram.

2.1. Feature extraction

Even though SIFT and ASIFT have proven to have a good performance [2], in our experiments using aerial images with a large number of repetitive patterns this was not the case. We found that SIFT could not find enough correspondences to create highly prominent peaks in the pixel-distance histograms, which difficult the identification of correct 2D translations. Therefore, we conducted a study to find the feature extractor and descriptor methods more suitable for our feature matching approach. We found that Oriented FAST and rotated BRIEF (ORB) extended with affine transformations [9], which we refer to as AORB, are best suited to use with images with a large number of repetitive patterns when the translation estimation approach is used. This is due to the fact that ORB has shown high and stable repeatability for matching images [7], which is reinforced when affine transformations are used. In addition, to minimize the noise present in pixel-distance histograms, the images are rectified using the intrinsic camera parameters.

2.2. Feature matching

After computing features using AORB, feature matching between image pairs, a query image (I_q) and a reference image (I_r) with overlap, is performed using Hamming distance. To tackle the problem caused by local ambiguities, we compute the matching using multiple nearest neighbors as matching candidates, known as k -nearest neighbor matching. This process involves matching one feature from one image with k features from the other image in a pair.

Based on the premise that most correct correspondences are not the closest matches when a large number of repetitive patterns are present [6], this approach significantly increases the probability of finding correct matches. Of course, this approach also has a downside: it will introduce many false correspondences due to local ambiguities in addition to correct matches.

2.3. Geometric verification assisted by GPS data

The geometric verification is carried out in three steps: i) camera orientation estimation, ii) translation estimation, and iii) selection of the correct matching correspondences. As in [2], the 2D translation estimation is done by using pixel-distance histograms. However, we found that using the ratio test as a preliminary filter step results in less noisy histograms when many repetitive patterns are present compared to using the raw matches.

2.3.1. Camera orientation estimation

UAV images do not always have the same orientation. For example, in a zig-zag flight pattern where the UAV turns for capturing the subsequent row, images between consecutive rows are not aligned but rotated 180 degrees. This misalignment can be estimated during the matching process, taking the first image as the reference and labeling their matched pairs as aligned in the same direction or not with the reference. Subsequent pairs are labeled based on the pairs that have been already labeled. As in [2], a pixel-rotation histogram is employed to estimate if an image pair is aligned or not. However, we consider only two discrete rotation values: 0 degrees when the image pair is aligned and 180 degrees when not.

2.3.2. Translation estimation assisted by GPS data

To calculate the approximate pixel-translation for columns (d_x) and rows (d_y) between two images, the longitude and latitude coordinates are converted to x - and y -coordinates using a simple equirectangular projection which is reasonably accurate over small distances. Likewise, because the flight trajectory is not always rotationally aligned to the x - y plane, x - and y -coordinates are rotated to be aligned with respect to the flight trajectory. Therefore, the pixel-translation estimation d_x and d_y for columns and rows in an image pair (i, j) , can be calculated as follows:

$$d_x = G_x(y_r^j - y_r^i)q \quad d_y = G_y(x_r^j - x_r^i)q \quad (2)$$

where (x_r^i, y_r^i) and (x_r^j, y_r^j) , are the rotated coordinates of the image pair (i, j) , $q = 1$ when the camera orientation of the reference image is pointing to the positive x -coordinate and $q = -1$ when is pointing to the negative, and G_x and G_y is the ground sample distance (GSD) for the x - and y -coordinate, respectively.

Finally, the actual pixel-translation in rows (d_r^{ij}) and columns (d_c^{ij}) between an image pair (i, j) are identified as the closer localization of peaks in the pixel-distance histograms to d_x and d_y , respectively.

2.3.3. Selection of the correct matching correspondences

All matches between the image pair (i, j) obtained by k -nearest neighbor matching that have the same actual pixel-translation in rows (d_r^{ij}) and columns (d_c^{ij}) taken into account a certain threshold t are selected as the correct matches. This means that the correct matches should satisfy the following equation:

$$|\Delta_r^k - d_r^{ij}| \leq t \wedge |\Delta_c^k - d_c^{ij}| \leq t \quad (3)$$

where t should be larger or equal than the size of the bins d used to compute the pixel-translation histograms ($t \geq d$). A higher threshold t allows dealing with small camera misalignments to the flight path. Increasing t will increase the number of matches. However, it also will allow accepting more outliers as correct ones. To filter outliers present when a larger value t is used, we performed a post-filtering using RANSAC.

3. RESULTS

We evaluated our method using three datasets, one captured near a photo-voltaic (PV) power plant in Omuta (Japan), the other near a PV power plant in Piolenc (France), and the last one near a PV power plant in Sakai (Japan). All these datasets contain nadir-oriented images with a moderate and a high number of repetitive patterns. The Omuta dataset contains 21 images with a resolution of 4000x3000, the Piolenc dataset contains 42 images with a resolution of 4608x3456, whereas the Sakai dataset contains 22 images with a resolution of 5472x3648. In particular, the Piolenc dataset represents a very challenging scenario because all images contain repetitive patterns that cover almost the entire field of view. Fig. 1 shows an example of an image from each dataset. In our evaluation, the intrinsic camera parameters and the GPS data were known. A maximum of 43000 keypoints and features were extracted from each image using AORB. Matches were computed using 50 nearest neighbors and a bin size of 15 ($d = 15$) to create the pixel-distance histograms. Only images with at least 60% of overlap were matched.

We compared our results with those obtained by the method proposed in [2], labeled as KOCH, and the commercial software package Agisoft Metashape [1]. For this, we estimated the camera pose (location and rotation) using the matches obtained by our method and those obtained by Metashape and KOCH. Camera poses obtained were compared with the ground truth, which was acquired by manually matching the correspondences. If the difference between an estimated camera pose and the camera pose in the ground

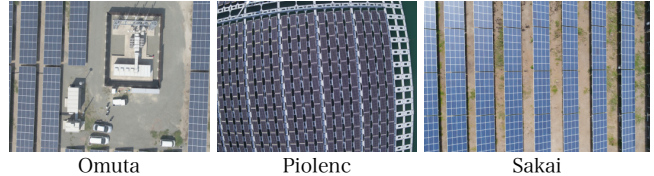


Fig. 1. Samples of images from each dataset. All of them contain repetitive patterns caused by solar panels in the pictures.

truth is less than a small threshold, the estimated camera pose is considered correct. Table 1 shows the results obtained from this evaluation. As expected, when a large number of repetitive patterns are present, as in the Piolenc dataset, local and global ambiguities cause the camera pose estimation in Metashape and KOCH to fail. As can be seen, matches obtained from the proposed method can be used to correctly estimate all the camera poses, even if images contain many repetitive patterns such as solar panels.

Dataset	Number of correct camera poses		
	Agisoft Metashape	KOCH [2]	Proposed
Omuta	42/42	41/42	42/42
Piolenc	3/21	0/21	21/21
Sakai	22/22	0/22	22/22

Table 1. Results of the comparison between the number of correct camera-poses computed using matches obtained from our proposed method and those obtained by Agisoft Metashape and KOCH [2].

Additionally, for the Piolenc and Sakai datasets we compute the orthomosaic generated using the camera position from both Metashape and our proposed method. As can be seen in Fig. 2, wrong camera position estimations for Piolenc in Metashape result in a wrong orthomosaic. Unlike Metashape, a complete and high-quality orthomosaic can be generated using the camera positions estimated from the matches generated by our proposed method. Likewise, as can be observed in Fig. 3, they do not present annoying artifacts (edge of solar panels) mainly created by small camera misalignments that happen in Metashape.

4. CONCLUSIONS

The experiments show that our proposed method can correctly estimate feature matches of nadir-oriented UAV images with many repetitive patterns. It assumes that the set of correct matches only differ in a 2D translation. Although this assumption limits the applicability of our approach, we plan to explore its extension with other types of UAV images. In addition, our proposed method uses ORB extended with affine transformations (AORB), which is free to use and showed im-

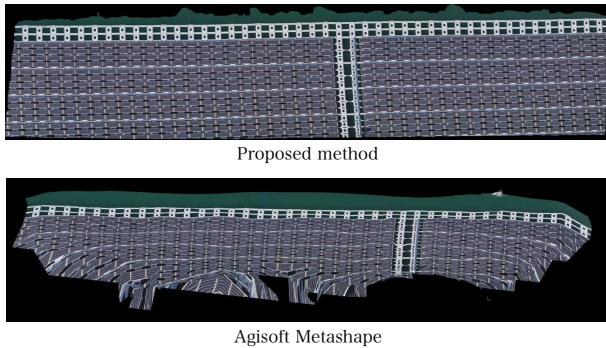


Fig. 2. Orthomosaics generated with the matches found by our proposed method (top) and Agisoft Metashape (bottom) for Piolenc. Our method generates matches that can be used to successfully reconstruct an accurate orthomosaic with highly repetitive patterns.

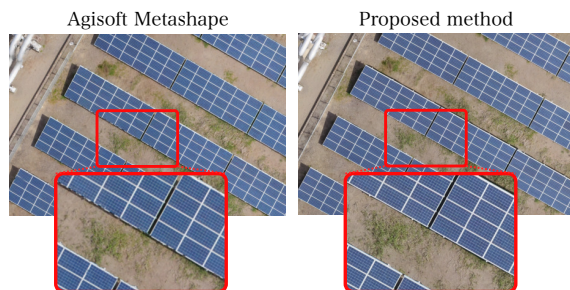


Fig. 3. A close-up view of the orthomosaics generated with the matches found by our proposed method and Agisoft Metashape.

proved performance on matching images that contain many repetitive patterns. Likewise, its use as a feature descriptor makes the matching process much faster, and it becomes an efficient alternative to SIFT.

By selecting the closer localization of peaks in the pixel-distance histograms, our approach allows dealing with not-accurate GPS data equipped on most operational UAVs. We found that it can remove outliers from local and global ambiguities, which helps to generate a more precise and complete orthomosaic. Using the more expensive and more precise differential GPS sensors can further improve to solve the ambiguities. A major drawback of our method is that large inconsistencies in GPS data and significant differences in angular or spatial sampling might introduce errors in the translation estimation. We are planning as future work to include additional steps in our approach and include new datasets that consider these situations.

5. ACKNOWLEDGMENT

This work was financially supported by the following projects: ANALYST-PV, Flanders Innovation & Entrepreneurship

project nr. HBC.2019.0050; COMP4DRONES ECSEL Joint Undertaking (JU) under grant agreement No 826610. The work of G. Luzardo is partially supported by Secretaría de Educación Superior, Ciencia, Tecnología e Innovación (SENESCYT) and Escuela Superior Politécnica del Litoral (ESPOL).

References

- [1] Agisoft Metashape. <https://www.agisoft.com/>, 2020. Accessed: 2020-01-07.
- [2] T. Koch, X. Zhuo, P. Reinartz, and F. Fraundorfer. A new paradigm for matching uav-and aerial images. *IS-PRS Annals of the Photogrammetry, Remote Sensing and Spatial Information Sciences*, 2016, 3:83–90, 2016.
- [3] C. Le Brese, C. N. Young, and J. J. Zou. A robust match filtering algorithm for use with repetitive patterns. In *2013, 7th International Conference on Signal Processing and Communication Systems (ICSPCS)*, pages 1–6. IEEE, 2013.
- [4] T. Lin and X. Wang. Hierarchical clustering matching for features with repetitive patterns in visual odometry. *Journal of Intelligent & Robotic Systems*, 100(3):1139–1155, 2020.
- [5] C. Stöcker, F. Nex, M. Koeva, and M. Gerke. High-quality uav-based orthophotos for cadastral mapping: Guidance for optimal flight configurations. *Remote Sensing*, 12(21):3625, 2020.
- [6] F. Sur, N. Noury, and M.-O. Berger. Image point correspondences and repeated patterns. Research Report RR-7693, INRIA, July 2011.
- [7] S. A. K. Tareen and Z. Saleem. A comparative analysis of sift, surf, kaze, akaze, orb, and brisk. In *2018 International conference on computing, mathematics and engineering technologies (iCoMET)*, pages 1–10. IEEE, 2018.
- [8] C. Wei, H. Xia, and Y. Qiao. Fast unmanned aerial vehicle image matching combining geometric information and feature similarity. *IEEE Geoscience and Remote Sensing Letters*, 2020.
- [9] G. Yu and J.-M. Morel. Asift: An algorithm for fully affine invariant comparison. *Image Processing On Line*, 1:11–38, 2011.
- [10] Z. Yu, H. Zhou, and C. Li. Fast non-rigid image feature matching for agricultural uav via probabilistic inference with regularization techniques. *Computers and Electronics in Agriculture*, 143:79 – 89, 2017.